IEEE Access
Multidisciplinary | Rapid Review | Open Access Journal

Received October 11, 2018, accepted October 21, 2018, date of publication October 25, 2018,
date of current version November 30, 2018.

Digital Object Identifier 10.1109/ACCESS.2018.2877960

Hierarchical Braking Torque Control of In-Wheel-Motor-Driven Electric Vehicles Over CAN

WEI LI[1], XIAOYUAN ZHU[2], AND JI JU[3]
[1]School of Logistical Engineering, Shanghai Maritime University, Shanghai 201306, China
[2]Merchant Marine College, Shanghai Maritime University, Shanghai 201306, China
[3]College of Information Engineering, Shanghai Maritime University, Shanghai 201306, China

Corresponding author: Xiaoyuan Zhu (xyzhu@shmtu.edu.cn)

This work was supported in part by the National Natural Science Foundation of China under Grant 51605278 and Grant 51605279, in part by the Shanghai Education Development Foundation through the Chenguang Program, and in part by the Shanghai Municipal Education Commission under Grant 16CG54.

ABSTRACT This paper proposes a hierarchical braking torque control system design over controller area network (CAN) for electric vehicle with four in-wheel motors. Based on nonlinear tyre-road friction estimation, an adaptive braking torque control scheme is devised in the upper level controller to simultaneously regulate the wheel slip ratio for both front and rear wheels. While in the lower-level controller, a frequency-depended braking torque allocator is developed to dynamically distribute the braking torques command from upper level controller into friction braking torque and regenerative braking torque. A braking supervisor is established to enable or disable proposed hierarchical braking controller according to wheel slip ratio as well as vehicle speed condition. To avoid undesired discontinuities in braking torque signal when proposed braking controller is enabled abruptly, an initial value of the estimated tyre-road friction is rescaled additionally. Dedicated CAN bus module is built by using SimEvent toolbox, by which vehicle states as well as control signals can be transmitted and shared. Co-simulation by using MATLAB/Simulink and CarSim is conducted to demonstrate the effectiveness of the proposed hierarchical braking torque controller. Random CAN-induced delays are considered in the braking control process, by which the robustness of the proposed hierarchical braking controller is further verified.

INDEX TERMS Hierarchical braking torque control, adaptive braking control, braking torque allocation, CAN-induced delays, electric vehicle with four in-wheel motors.

I. INTRODUCTION

Braking control is very important to the vehicle control performance, which is directly related with the active safety of vehicle system. From anti-lock braking system (ABS) to vehicle dynamic control (VDC), research on braking system is always a hot topic [1], [2]. Due to inherent high nonlinearity of tyre-road friction as well as braking dynamical model, controller design for braking system is generally complex and challenging. Furthermore, vehicle electrification has brought great changes to the architecture of the vehicle powertrain system, which also brings many benefits to the vehicle braking system. The first one is the regenerative braking capability, which can convert kinetic energy of the vehicle into electric energy so as to increase the driving range. The other one is the fast and accurate dynamic characteristic of electric machine, which can bring promising potential in braking control performance improvement. Therefore, regenerative braking system is generally working together frictional braking system and playing an increasingly important role in the vehicle braking process. However, before enjoying the benefit of electric motor in the braking system, good cooperation between friction brakes system and electric motor must be ensured first, which further complicates the controller design work for braking system.

For both traditional engine vehicles and electric vehicles, two strategies are generally used in the braking torque control [3]. The first one is wheel deceleration based method, in which vehicle speed information is not required and braking torque is adjusted by using wheel deceleration thresholds triggered on/off switching [4]. When vehicle speed can be measured or estimated, wheel slip ratio based braking torque control is used as the second approach [5]. Compared with

wheel deceleration based braking torque control, wheel slip ratio based method is generally preferred, as the tyre-road contact information can be better used to improve the braking performance. And there are also some composite braking torque control approaches in which wheel deceleration based method and wheel slip ratio based method are combined together [6]. For wheel slip ratio regulation, many control methods including sliding mode control [1], [5], [7], robust control [3], [8], fuzzy control [9], [10], model predictive control [11] and gain scheduling approach [12], etc., have been discussed. And the sliding mode control, as a nonlinear control technique, is the most popular one due to its low sensitivity to system parameter variations and disturbances, while easy tuning and implementation. In order to better handle the parametric uncertainty in the tyre-road friction as well as continuous vehicle velocity change, adaptive mechanisms are expected to be further explored and incorporated in the braking controller design.

For electric vehicles, as both frictional braking system and driving motors are involved in the braking process, coordination between these two braking system must be addressed in the braking actuator level for each wheel [13]. A co-operative control algorithm for regenerative braking and frictional braking is proposed to prevent wheel lock, by which desired road friction coefficient can be better maintained while the regenerative braking duration can be also extended to increase energy recovery [14]. Considering the effect of downshift to the braking process, a cooperative control algorithm is further proposed for frictional braking and regenerative braking to maintain desired braking force and driving comfort [15]. Considering damping as well as elastic properties of electrified powertrains, a blended braking control algorithm using extended Kalman filter (EKF) is proposed to enhance the braking performance and energy efficiency [16]. For electric vehicle with in-wheel motors, braking torque allocation can be realized in flexible and diversified ways. Huang and Wang [17] proposed a braking toque allocation scheme for electric vehicle with four in-wheel motors, in which only regenerative braking is considered and nonlinear model predictive control approach is used to regulate the wheel slip ratios and distribute the braking torque between front and rear in-wheel motors. Wang *et al.* [18] further proposed a torque allocation scheme electric vehicle with four in-wheel motors, in which both friction braking system and regenerative braking system are considered. In this braking allocation scheme, the frictional braking torque value is fixed during the braking process while the regenerative braking torque is used to compensate the difference between frictional baking torque and overall desired braking torque. This allocation scheme is relatively simple but effective, which can make good use of fast dynamic response of in-wheel motors during braking process. de Castro *et al.* [19] presented a hybrid ABS solution for electric vehicles with in-wheel motors, in which robust adaptive wheel slip ratio control approach, and torque blending method between mechanical braking and electric braking system are proposed to optimize energy efficiency and dynamic performances of the braking system. As this approach is only based on quarter car model, it can be further extended to full vehicle model, by which weight transfer effect between front and rear wheels can be better considered. With the development of intelligent vehicle as well as transportation, brake-by-wire is emerged as a promising braking control scheme in modern vehicles [20]. By using communication network such as CAN, the brake-by-wire system offers easy connection with other vehicle control system. However, due to the physical bandwidth limitation of the communication network, and increasing information exchange requirement for vehicle-to-vehicle (V2V), vehicle-to-infrastructure (V2I), and vehicle-2-X (V2X) technology [21], [22], random network-induced delays, packet loss, and even congestion are more likely to appear, which could degrade the performance or even destabilize the vehicle control system [23], [24]. Though the braking signal is generally designed to have the highest priority in the vehicle network, it is still necessary to improve the robustness of the braking control system or at least evaluate the effect of possible network-induced problems to the braking control performance.

In this paper, a hierarchical braking torque controller design is proposed for electric vehicle with four in-wheel motors. A robust adaptive wheel slip ratio controller is developed in the upper-level, while frequency-depended braking torque allocator is presented in the lower-level. The main contributions of this paper lie in the following aspects

1) Instead of tyre-road friction estimation, tyre-road friction is directly estimated to handle the parameter uncertainties and the weight transfer phenomena during braking process. And based on vehicle single-track model, braking torque allocation between both front/rear wheels and frictional/regenerative brake systems are addressed simultaneously.
2) Network-induced random delays modeled by using SimEvent toolbox is considered in the braking control system, by using which the robust performance of proposed hierarchical braking controller is further verified.

The rest of this paper is as follows: In Section 2, problem formulation as well as dynamical modeling are presented. Adaptive braking torque controller design in the upper-level is presented in Section 3. Frequency-depended braking torque allocator in the lower-level is presented subsequently presented in Section 4. Co-Simulation results based on MATLAB/Simulink and CarSim are presented in Section 5 and concluding remarks are summarized in Section 6.

II. PROBLEM FORMULATION

A. ARCHITECTURE OF THE HIERARCHICAL BRAKING CONTROL SYSTEM

The proposed hierarchical braking torque control system is shown in Figure 1. An adaptive braking torque controller is established as the upper-level controller, which will regulate the wheel slip ratio of both front and rear wheels to make full use of the available tyre-road friction. While in the lower-level controller, a frequency-depended braking torque

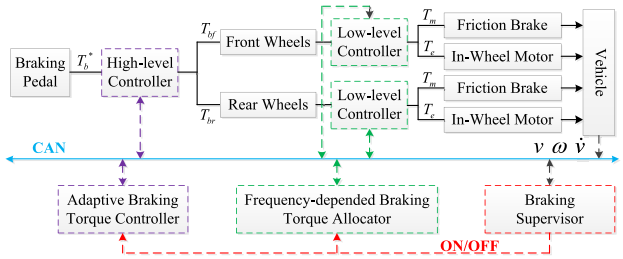

FIGURE 1. Scheme of the proposed hierarchical braking torque control system.

allocator is developed to distribute the braking torque into frictional brake torque and regenerative braking torque. During the braking process, a braking supervisor is established to enable or disable proposed hierarchical braking controller according to wheel slip ratio as well as vehicle speed condition. Controller Area Network (CAN) is adopted in proposed hierarchical braking torque control system, by which vehicle states as well as control signals can be transmitted and shared in different controllers conveniently. At the beginning of the braking process, the braking torque will be just linear to the brake pedal travel with predefined ratios, and proposed braking controller will not be activated until sudden wheel slip ratio change is detected in braking control supervisor. When the vehicle speed is continuously dropped below a certain value, the braking torque controller will be disabled by the braking control supervisor. And the frictional brake torque will be applied only to completely stop the vehicle.

B. VEHICLE LONGITUDINAL DYNAMICAL MODELING

It is supposed that the vehicle is decelerated in straight-line during the braking process. Thus, the vehicle single-track model shown in Fig 2 is adopted in this paper, where the load transfer phenomena between front and rear wheels can be described [1]. And braking torque allocation between frictional braking torque and regenerative braking in each wheel, as well as the braking torque distribution between front and rear wheels can be all considered.

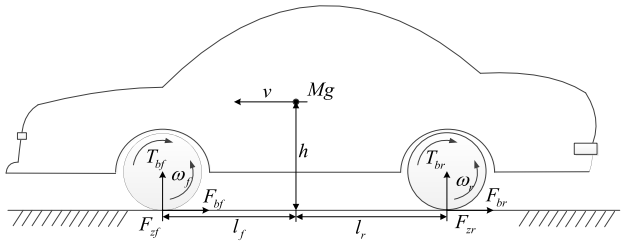

FIGURE 2. Vehicle single-track model.

According to Fig 2, dynamic model of the electric vehicle with four in-wheel motors can be derived as

$$\begin{aligned} \lambda_i &= \frac{v-\omega_i}{v}, \quad \sum F_{zi} = Mg \\ M\dot{v} &= -r_w \sum \left(\mu\left(\lambda_i\right) F_{zi}\right) - \Delta\left(v\right) \\ J\dot{\omega}_i &= r_w \mu\left(\lambda_i\right) F_{zi} - T_{bi} - \Delta\left(\omega\right), \quad i \in \{f, r\} \end{aligned} \tag{1}$$

where v and ω are the vehicle speed and wheel speed respectively, λ is the wheel slip ratio, F_Z is the wheel vertical load, M is half the mass of vehicle, r_w is the wheel radius, μ is the nonlinear tyre-road friction coefficient which is related to wheel slip ratio, J is the wheel inertia, T_b is the braking torque, $\Delta(v)$ and $\Delta(\omega)$ are the disturbance force and torque, subscript f and r indicate the front and rear wheel respectively.

C. CALCULATION OF THE TYRE-ROAD FRICTION

As the braking toque to be controlled is directly decided by the tyre-road friction, both wheel vertical loads and tyre-road friction coefficients need to be obtained in the braking control process. When the vehicle deceleration signal is available, the wheel vertical loads can be directly calculated as,

$$\begin{aligned} F_{zf} &= \frac{Mg}{l_f + l_r}(l_f - \frac{\dot{v}}{g}h) \\ F_{zr} &= \frac{Mg}{l_f + l_r}(l_r + \frac{\dot{v}}{g}h) \end{aligned} \tag{2}$$

where l_f is the distance between the centre of gravity and the front axle, l_r is the distance between the centre of gravity and the rear axle, h is the height of vehicle's gravity centre.

The tyre-road friction coefficient is generally the major source of parametric uncertainty as well as system nonlinearity in the braking control system design, which is described by using Burckhardt model as

$$\mu\left(\lambda\right) = c_1(1 - \exp(-c_2\lambda)) - c_3\lambda \tag{3}$$

where $c_i, i = 1 \sim 3$ are the parameters of the Burckhardt tyre model.

The friction co-efficient values in equation (3) for different road conditions can be identified by using vehicle test data. For typical roads, the parameter sets in Table 1 are widely adopted [25].

TABLE 1. Parameters set for typical Burckhardt tire model.

Road type	c1	c2	c3
Asphalt, dry	1.281	23.99	0.52
Asphalt, wet	0.857	33.822	0.347
Concrete, dry	1.1973	25.168	0.5373
Snow	0.1946	94.129	0.0646

In order to deal with the exponential term in the Burckhardt tyre model, Linear Parameterization (LP) approximation approach is adopted. And the coefficients in equation (3) are rearranged as

$$\begin{aligned} \mu\left(\lambda\right) &= c_1 - c_3\lambda - c_1\exp(-c_2\lambda)) \\ c_1 &= \varphi_1, -c_3 = \varphi_2, c_1\exp(-c_2\lambda) \approx \sum_{i=1}^{n} \varphi_{i+2}\exp(-\alpha_i\lambda) \end{aligned} \tag{4}$$

where $\varphi_i, i = 1 \sim n$ are the approximated linear parameters, and α_i are the related fixed weights.

Thus, the tyre-road friction model can be further simplified as

$$\mu(\lambda) = \varphi^T \Phi(\lambda) + \Delta(\lambda)$$
$$\Phi(\lambda) = [\,1 \quad \lambda \quad e^{-\alpha_1\lambda} \quad e^{-\alpha_2\lambda} \quad e^{-\alpha_3\lambda}\,]^T \tag{5}$$

where φ is a set of linear coefficient values, $\Phi(\lambda)$ is the regression term with fixed structure, and $\Delta(\lambda)$ is the approximation error.

In order to show the fitting performance of the LP approximation approach, comparative analysis is conducted. For dry asphalt road, the parameter sets in Burckhardt tyre model is chosen as $c = [\,1.281\ 23.99\ 0.52\,]^T$, while the regression term in LP approximation model is set as $\Phi(\lambda) = [\,1\ \lambda\ e^{-4.99\lambda}\ e^{-18.43\lambda}\ e^{-65.62\lambda}\,]^T$ [26]. The comparative result can be seen in Fig 3, where the fitting errors between proposed PL approximation model and standard Burckhardt tyre model are quite small. For the parameter uncertainty in φ caused by the approximation error $\Delta(\lambda)$, adaptive mechanisms will be further incorporated in the next section to handle this problem. Due to the weight transfer phenomena, the vertical forces of front and rear tires are dynamically changed during the braking process. Thus, the braking torque should be adjusted accordingly to simultaneously regulate the slip ratios of front and rear wheels to their desired values.

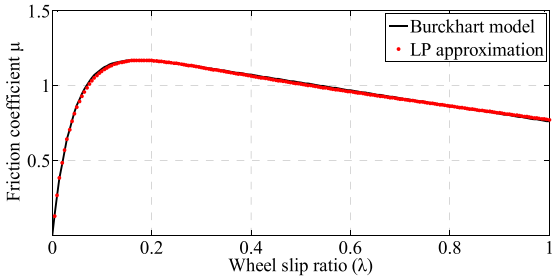

FIGURE 3. Fitting performance of Linear Parameterization (dry asphalt).

III. ADAPTIVE BRAKING TORQUE CONTROLLER DESIGN

The major control target of the upper-level control is to design an adaptive braking torque control law to maintain the wheel slip ratio of both front and rear wheels to the desired value as fast as possible. In order to precisely control the brake torque, the tyre-road friction of each wheel must be obtained. However, as tyre-road friction coefficients are highly nonlinear with the wheel slip ratio, and the wheel vertical load is also dynamically changed in each wheel due to the weight transfer phenomena, both of them are difficult to be obtained accurately. Therefore, instead of tyre-road friction estimation, it is better to estimate the tyre-road friction directly.

A. ADAPTIVE WHEEL SLIP RATIO REGULATION

As the disturbance force $\Delta(v)$ and torque $\Delta(\omega)$ in equation (1) is generally bounded and can be neglected, the first deviation of wheel slip ratio can be approximately described as

$$\dot{\lambda}_i = \frac{\partial h}{\partial v}\dot{v} + \frac{\partial h}{\partial \omega_i}\dot{\omega}_i,\ i \in \{f, r\}$$
$$= -\frac{r_w}{Jv}\left(\left(1 + (1-\lambda_i)\frac{J}{Mr_w^2}\right) r_w \mu(\lambda_i) F_{zi} - T_{bi}\right) \tag{6}$$

Considering the wheel inertia is usually much smaller than equivalent vehicle inertia Mr_w^2, equation (6) can be further simplified as

$$\dot{\lambda}_i = -\frac{r_w}{Jv}\left(r_w \mu(\lambda_i) F_{zi} - T_{bi}\right), \quad i \in \{f, r\} \tag{7}$$

The desired wheel slip ratio is set to be λ^*, and the wheel slip ratio regulation error can be defined as

$$e_i = \lambda_i - \lambda_i^*, \quad i \in \{f, r\} \tag{8}$$

Based on equation (7), the error dynamics of the wheel slip ratio can be defined as

$$\dot{e}_i = -\frac{r_w}{Jv}(r_w \mu(\lambda_i) F_{zi} - T_{bi}), \quad i \in \{f, r\} \tag{9}$$

Subsisting equation (5) into (9) and neglecting the LP approximation error term $\Delta(\lambda)$, the error dynamics of the wheel slip ratio can be rewritten as

$$\dot{e}_i = -\frac{r_w}{jv}(r_w \varphi^T \Phi(\lambda_i) F_{zi} - T_{bi}), \quad i \in \{f, r\} \tag{10}$$

The adaptive braking torque control law is designed as

$$T_{bi} = r_w \varphi^T \Phi(\lambda_i) F_{zi} - v k_i e_i, \quad i \in \{f, r\} \tag{11}$$

where k_i are the positive tuning parameters for front and rear wheels.

Then, the error dynamics of the wheel slip ratio is changed into

$$\dot{e}_i = -\frac{r_w}{J} k_i e_i, \quad i \in \{f, r\} \tag{12}$$

Therefore, by using the braking control law in (10), both front and rear wheel slip ratio will exponentially converge to the desired value.

B. TYRE-ROAD FRICTION ESTIMATION

Before using the braking control law in (11), accurate tyre-road friction information is required to be estimated. Considering the structure of the regression term $\Phi(\lambda_i)$ is fixed after Linear Parameterization and can be known in advance, a new parameter is defined to handle the uncertain items φ and F_{zi} together as

$$\theta_i = \varphi F_{zi}, \quad i \in \{f, r\} \tag{13}$$

Thus, the tyre-road friction estimation can be finished by estimating the new defined parameter θ_i only, and the braking control law in (11) is changed into

$$T_{bi} = r_w \hat{\theta}_i^T \Phi(\lambda_i) - v k_i e_i, i \in \{f, r\} \tag{14}$$

Then the error dynamics of the wheel slip ratio in (10) is converted as

$$\dot{e}_i = -\frac{r_w}{J} k_i e_i + \frac{r_w^2}{Jv}(\hat{\theta}_i - \theta_i)^T \Phi(\lambda_i), \quad i \in \{f, r\} \tag{15}$$

The adaption law to estimate θ_i is designed as

$$\hat{\theta}_i(t) = \hat{\theta}_i(t_0) - \int_{t_0}^{t} \gamma_i \frac{e_{\varepsilon i}(\tau)}{v(\tau)} \Phi(\lambda_i(\tau))\, d\tau$$
$$e_{\varepsilon i} = \begin{cases} 0 & if\ |e_i| < \varepsilon_i \\ e_i - \varepsilon_i sgn(e_i) & if\ |e_i| \geq \varepsilon_i, \end{cases} \quad i \in \{f, r\} \tag{16}$$

where $e_{\varepsilon i}$ are the wheel slip regulation errors with dead zone ε_i for front and rear wheels, and γ_i are the constant tuning parameters of front and rear wheels.

Considering following candidate Lyapunov function

$$V\left(e_{\varepsilon i}, \tilde{\theta}\right) = \frac{1}{2} e_{\varepsilon i}^2 + \frac{r_w^2}{2\gamma_i J} \tilde{\theta}_i^T \tilde{\theta}_i$$
$$\tilde{\theta}_i = \hat{\theta}_i - \theta_i, \quad i \in \{f, r\} \tag{17}$$

Then, the stability of the wheel slip ratio error dynamics can be ensured. And the proof process can be finished by following a similar way in [19].

C. ADAPTIVE BRAKING TORQUE CONTROLLER INITIALIZATION DESIGN

At the beginning of the braking process, the braking torque T_b is directly decided by the pedal travel. When excessive wheel slip ratio change is detected by the braking control supervisor, the adaptive braking torque controller is enabled immediately. Thus, the braking torque generated by the adaptive braking torque controller may be not equal to the braking torque $T_b(t_s)$ that is decided by the pedal travel at the switching moment t_s. These discontinuities in the braking torque signal may bring longitudinal shock during the braking process, which will largely decrease the ride comfort of the vehicle.

In order to avoid these undesired discontinuities when the adaptive braking torque controller is enabled, initial value of θ'' is rescaled as

$$\hat{\theta}_i(t_s) = \theta_i \frac{T_b(t_s) + k_i v(t_s) e_i(t_s)}{\theta_i^T(t_s)\Phi(\lambda_i(t_s))}, \quad i \in \{f, r\} \tag{18}$$

IV. FREQUENCY-DEPENDED BRAKING TORQUE ALLOCATION

A. DYNAMICAL MODELING OF BRKAING ACTUATORS

In order to show the torque response difference of the frictional braking system and regenerative braking system, first-order system with delay are adopted as

$$\frac{T_j}{T_j^*}(s) = \frac{1}{1 + \tau_j s} \exp(\delta_j s), \quad j \in \{m, e\} \tag{19}$$

where T_j^* is the reference braking torque, T_j is the actual output braking torque, τ_j is the dominant time constant, δ_j is the pure system delay, T_m and T_e are the mechanical brake torque generated by frictional braking system and electric brake torque generated by in-wheel motor respectively

As the dynamical response of the in-wheel motors is generally much faster than that of frictional braking system actuated by electro-hydraulic or electro-mechanic system, τ_e will be accordingly much smaller than τ_f.

Considering the physical constraint on friction braking system and in-wheel motor, the ranges and rates of mechanical and electric braking torque are respectively constrained as

$$T_{j,\min} \leq T_j \leq T_{j,\max}, j \in \{m, e\} - \dot{T}_{j,\max} \leq \dot{T}_j \leq \dot{T}_{j,\max} \tag{20}$$

B. BRAKING TORQUE ALLOCATION DESIGN

Based on the different dynamical response of frictional braking system and regenerative braking system, the major idea of proposed braking torque allocation scheme is that the in-wheel motor should be more sensitive to the high-frequency brake torque command that from upper-level controller. Thus, a frequency-depended braking torque allocation ratio is defined as

$$\rho(f_b) = |T_e / T_m| \tag{21}$$

where f_b is the frequency of the braking torque signal.

It should be noted that no matter how the allocation ratio varies, following equation must be satisfied as

$$T_b = T_m + T_e \tag{22}$$

By using forward Euler method, the variation rate of braking torque can be approximated as

$$\dot{T}_j = \left(T_j[k] - T_j[k-1]\right)/t_s, \quad j \in \{m, e\} \tag{23}$$

where t_s is the sampling period.

In order to further pursue the benefit of the torque allocation, following optimization problem are then formulated to minimize the brake torque requirement as

$$\min_{T_m, T_e} \Big\{ (\alpha_m T_m^2 + \alpha_e T_e^2) + \left(\beta_m \left(T_m - T_m[k-1]\right)^2 + \beta_e \left(T_e - T_e[k-1]\right)^2\right) \Big\}$$
$$s.t.\ T_m + T_e = T_d, T_j \leq T_j \leq \bar{T}_j, j \in \{m, e\}$$
$$T_j = \max\left\{T_{j,\min}, T_j[k-1] - t_s \dot{T}_{j,\max}\right\}$$
$$\bar{T}_j = \min\left\{T_{j,\max}, T_j[k-1] + t_s \dot{T}_{j,\max}\right\} \tag{24}$$

where α_m, α_e, β_m, β_e are different weighting factors to be designed.

The first part of the cost function in (24) is used to optimize the amplitudes of both frictional braking torque and regenerative braking torque. And the second part is used to constraint the variation rate of braking torque for each braking actuator. By using the forward Euler method in (23), the variation rate constraints of the braking torque are converted into range constraints. Thus, the number of inequalities constraints can be reduced.

In order to solve the optimization problem in (24), following Lagrangian function is defined as

$$L(T_m, T_e, \ell)$$
$$= \alpha_m T_m^2 + \alpha_e T_e^2 + \beta_m \left(T_m - T_m[k-1]\right)^2 + \beta_e \left(T_e - T_e[k-1]\right)^2 + \ell_L \left(T_m + T_e - T_b\right) \tag{25}$$

where ℓ_L is Lagrange multiplier.

Applying the following first-order conditions

$$\begin{aligned}\frac{\partial L}{\partial T_m} &= 2\alpha_m T_m + 2\beta_m \left(T_m - T_m\left[k-1\right]\right) + \ell_L = 0\\ \frac{\partial L}{\partial T_{\mathrm{e}}} &= 2\alpha_{\mathrm{e}} T_{\mathrm{e}} + 2\beta_{\mathrm{e}} \left(T_{\mathrm{e}} - T_{\mathrm{e}}\left[k-1\right]\right) + \ell_L = 0\\ \frac{\partial L}{\partial \ell_L} &= T_m + T_e - T_{\mathrm{b}} = 0 \end{aligned} \tag{26}$$

By solving the equations in (26), following discrete time filters can be obtained as

$$\begin{aligned}\frac{T_m}{T_b}(z) &= \frac{\alpha_e + \beta_e}{l}\frac{z - \beta_e/(\alpha_e + \beta_e)}{z - (\beta_m + \beta_e)/l}\\ \frac{T_e}{T_b}(z) &= \frac{\alpha_m + \beta_m}{l}\frac{z - \beta_m/(\alpha_m + \beta_m)}{z - (\beta_m + \beta_e)/l}\\ l &= \alpha_m + \alpha_e + \beta_m + \beta_e \end{aligned} \tag{27}$$

where z is the Z-transform operator

By using the discrete filters in (27), the braking torque command from the high-level controller can be dynamically distributed between frictional braking system and regenerative braking system.

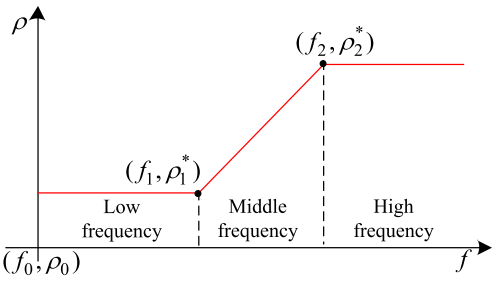

FIGURE 4. Desired braking torque allocation ratio.

As it is shown in Fig 4, according to different frequency values, the desired torque allocation ratio can be dynamically adjusted. If the frequency value of the braking torque command is very high, the torque allocation ratio will kept in a large value to make full use of the regenerative braking. While in the low frequency zone, the torque allocation ratio will be reduced accordingly, which means frictional braking system will play the dominant role.

In order to generate a set of torque allocation ratios that can be close to the desired allocation ratio values shown in Fig 4, following nonlinear least squares problem is defined as

$$\min_{\alpha_m,\alpha_e,\beta_m,\beta_e} \sum_{k=1}^{n} \left(\rho_k^* - \rho\left(f_k\right)\right)^2 \tag{28}$$

where $k = 1, 2 \ldots, n$ is the number of sample points

By solving the nonlinear least squares problem in (28), a suitable set of torque allocator weights can be find to both fulfill the constraint requirements in (24) and also make the shape of actual braking torque allocation ratio curve be close to the desired one shown in Fig 4.

V. SIMULATION RESULTS AND ANALYSIS

As it is shown in Fig 5, co-simulations are conducted in MATLAB/Simulink to evaluate the performance of proposed hierarchical braking control strategy. The full car model is provided by CarSim. In the simulation model, there are mainly adaptive slip regulator (adaptive braking torque controller) module, braking torque allocation module, wheel slip calculation module, braking supervisor module and CAN bus module.

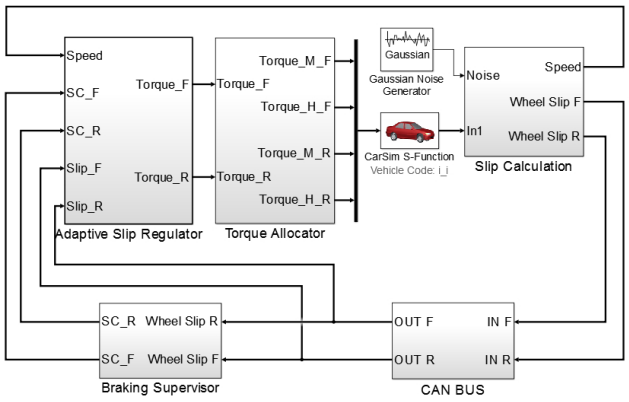

FIGURE 5. Co-Simulation model for proposed hierarchical braking torque control system.

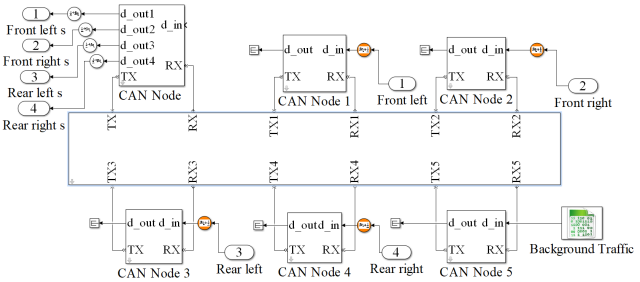

FIGURE 6. CAN bus module.

Detailed CAN bus model is built by using SimEvent toolbox, which is shown in Fig 6. The data loss rate is set to be 0.1% and transmission rate is 250 Kbit/s, which follow the suggestion of SAE J1939. There are 6 nodes in CAN Bus model with different priorities. Node 0 with the highest priority is for the braking controller. Node 1∼4 are for four wheel slip ratios. And Node 5 with the lowest priority is for the disturbance message, by using which random delays cam be produced in the CAN bus.

As it is shown in Fig 7, a typical E-class sedan in the CarSim library is selected as the test vehicle for the co-simulation. It is assumed that both front and rear wheels are equipped with disc brake. And the default brake system module in CarSim library is selected for all the wheels. The major parameters for the simulation are listed in Table 2.

First, it is assumed that there is no background traffic in CAN. Vehicle is decelerated in a straight way from 100 km/h. It can be seen from equation (10) that the slip error dynamics

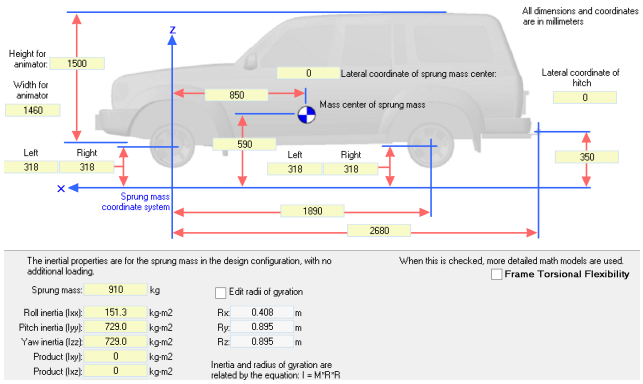

FIGURE 7. Vehicle model in CarSim.

TABLE 2. Parameters in the simulation.

Parameters	Value	Unit
Vehicle mass (M)	910	kg
Wheel inertia (J)	1.5	$kg.m^2$
Wheel radius (r)	0.3	m
Wheel base (l)	1.89	m
Distance between the centre of gravity and the front axle (l_f)	0.85	m
Distance between the centre of gravity and the rear axle (l_r)	1.04	m
Maximum electric torque (T_e)	200	Nm
Dead zone (ε)	0.005	-
Control gain of front wheel (k_f)	30	-
Control gain of rear wheel (k_r)	15	-
Adaptive rate of front wheel (γ_f)	800000	-
Adaptive rate of rear wheel (γ_r)	5000000	-
Time constant of mechanical brake (τ_m)	0.016	s
Dead time of mechanical brake (δ_m)	0.015	s
Time constant of electric brake (τ_e)	0.0015	s
Dead time of electric brake (δ_e)	0.00005	s
Initial vehicle speed (v_0)	100	km/h
Vehicle speed threshold (v_s)	5	km/h
Initial value of the linear coefficient set (φ)	$[1.22\ -0.45\ 0.18\ -1.19\ -0.25]^T$	-
Weighting factors ($[\alpha_m\ \ \alpha_e\ \ \beta_m\ \ \beta_e]$)	$[0.002\ 0.005\ 0.8\ 0.2]^T$	-

will be too fast to control in engineering practice when vehicle velocity approaching zero. And it is not cost-effective to use regenerative braking during low speed condition. Thus, when the vehicle speed is below 5km/h, the proposed braking torque control system will be disabled. Only the frictional braking torque will be applied and both wheels will be totally locked. According to Fig 3, the desired slip ratio is set as 0.16 for both front and rear wheels. In order to consider the negative effect of inevitable measurement errors, Gaussian noise with variance 0.005 is added in the wheel slip ratio signal.

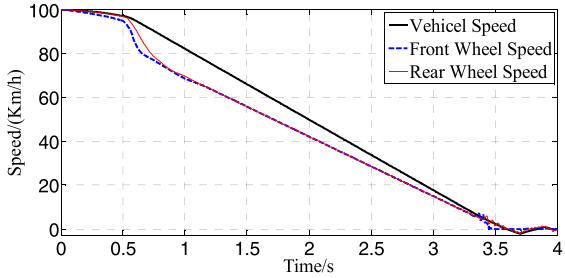

FIGURE 8. Wheel and vehicle speed response.

It can be seen from Fig 8 that, by using proposed hierarchical braking torque control system, the speed responses of both front wheels and rear wheels are quite well during the braking process. The wheel rotation speeds of both front and rear wheels are well regulated simultaneously. Thus, desired wheel slip ratio can be maintained for all the wheels to make full use of the available tyre-road friction. When the vehicle's speed is less than 5km/h, the adaptive braking controller is disabled. And the vehicle comes to a complete stop at around 3.5s.

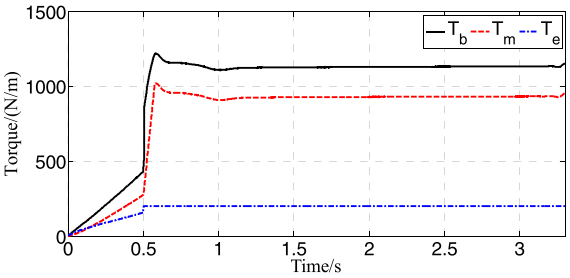

FIGURE 9. Torque allocation result of front wheel.

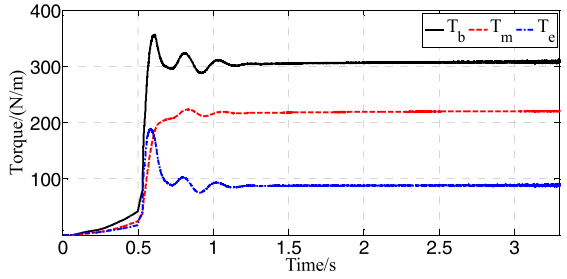

FIGURE 10. Torque allocation result of rear wheel.

The braking torque responses of front wheels and rears wheel are shown in Fig 9 and Fig 10 respectively. The braking torque of the front wheel is generally greater than that of rear wheel, which is mainly caused by the weight

transfer effect. In the beginning of the braking process, the braking torque output of the both front and rear wheel are just linear to the brake pedal travel. The adaptive braking torque controller is enabled at around 0.5s when excessive slip ratio change is detected. By using the braking torque allocator, both frictional and electric braking torques are dynamically distributed. And the torque amplitudes of all the in-wheel motors can be well constrained.

In order to better show the performance of the proposed hierarchical braking torque controller, traditional PI controller is used for comparative analysis. In the beginning of the braking process, the braking torque output is just linear to the brake pedal travel. Proposed controller and PI controller will be all enabled at around 0.5s when excessive slip ratio change is detected. The wheel slip ratio results can be seen in Fig 11. Compared with the traditional PI controller, proposed hierarchical braking torque controller can regulate the wheel slip ratio more smoothly during the whole braking process, especially in the moment when the braking controller is first initialized. And the PI controller would result large oscillation in the controller initialization process.

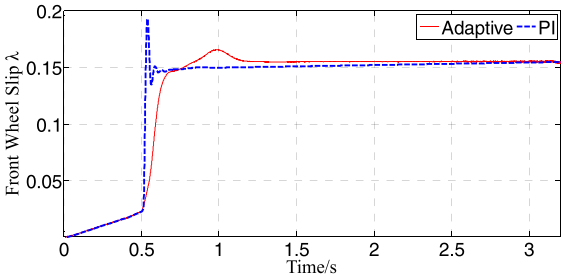

FIGURE 11. Wheel slip ratio regulation performance comparison.

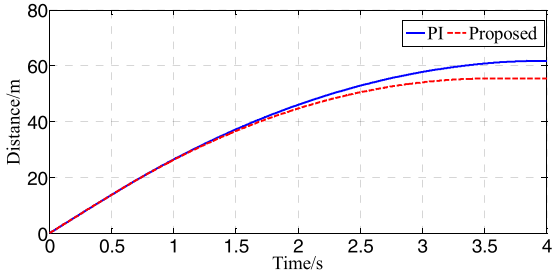

FIGURE 12. Brake distance comparison.

The braking distance results of the both braking controllers can be seen in Fig 12. Compared with traditional PI controller, the proposed hierarchical braking torque controller can offer shorter braking distance due to better wheel slip ratio regulation.

In order to further evaluate the robust performance of proposed hierarchical braking torque controller, effects of the CAN-induced delay on proposed hierarchical braking controller is evaluated. By turning on the disturbance message in Node 5, random delays in Node 1∼4 are show in Table 3.

TABLE 3. Message Transmission delays in CAN.

Nodes	Delays	Unit
CAN Node1	0.425	ms
CAN Node2	0.904	ms
CAN Node3	1.356	ms
CAN Node4	1.808	ms

It can be seen that Node 1 with highest priority has the smallest delay, while Node 4 with lowest priority has the largest message delay. And the message delay that induced by CAN in different nodes will be varied from 0.4ms to 1.8ms.

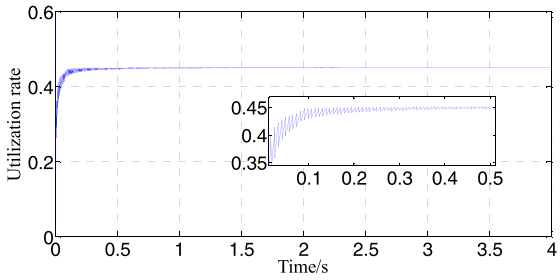

FIGURE 13. CAN BUS Utilization.

The load rate of the CAN bus is shown in Fig 13. The load rate of the CAN bus is gradually increased and finally stabilized at 0.45. As the CAN bus is not fully occupied by the braking controllers, it still can be used by other vehicle nodes for signal transmission.

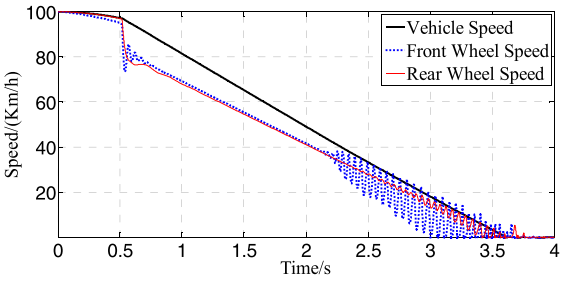

FIGURE 14. Speed response of traditional PI controller with CAN-induced delay.

The vehicle speed and wheel speed responses can be seen in Fig 14 and Fig 15. Due to message delivery delays caused by network traffic, the traditional PI controller will cause severe oscillations in the both front and rear wheels at around 2.2s. While the proposed hierarchical braking torque controller can still ensure good wheel speed control performance in spite of CAN induced delays.

The wheel slip ratio response can be seen from Fig 16 and Fig 17, where similar result can be concluded. The traditional PI controller failed to regulate wheel slip ratio to its desired value due to the negative effect of the CAN-induced message delays. Starting from the moment 2.2s, both front and

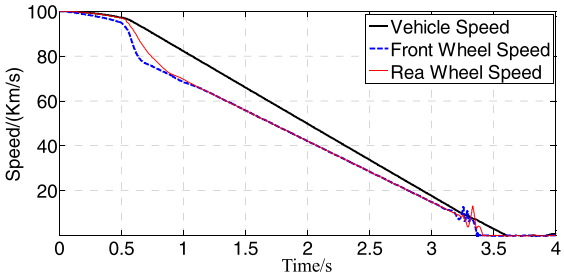

FIGURE 15. Speed response of proposed braking controller with CAN-induced delay.

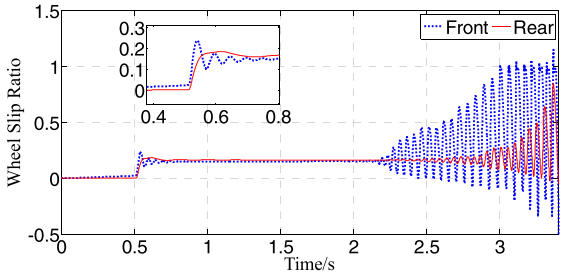

FIGURE 16. Wheel slip ratio response of traditional PI controller with CAN-induced delay.

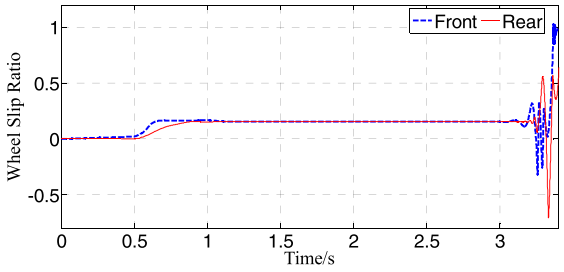

FIGURE 17. Wheel slip ratio response of proposed braking controller with CAN-induced delay.

rear wheel slip ratios are begin to oscillate more and more severely. It will make the vehicle system unstable and even in danger. However, good wheel slip ratio regulation performance can be still guaranteed by using proposed hierarchical braking torque controller.

VI. CONCLUSIONS

In this paper, a hierarchical braking torque control system design is proposed for electric vehicle with four in-wheel motors. By using adaptive feedback law, wheel slip ratio can be well regulated to its desired value for both front and rear wheels. And the proposed adaptive controller is also robust to friction uncertainties, measurement noise and message delivery delays caused by network traffic. By using a frequency-dependent allocation ratio, braking torque allocation can be realized in both front/rear wheels and frictional/regenerative braking systems simultaneously. Both the amplitudes and variation rates of these brake torques can be well constrained during the whole braking process. Braking supervisor is successfully incorporated in the proposed hierarchical braking torque control system, which can open or close both the wheel slip regulator in the upper-level and braking torque allocator in the lower-level according to different vehicle conditions, which can help better initialize the hierarchical braking controller to avoid undesired discontinuities in the braking torque output. The effectiveness of proposed braking controller is successfully verified by using co-simulation with Matlab/Simulink and CarSim.

REFERENCES

[1] X. Zhang, Y. Xu, M. Pan, and F. Ren, "A vehicle ABS adaptive sliding-mode control algorithm based on the vehicle velocity estimation and tyre/road friction coefficient estimations," *Vehicle Syst. Dyn.*, vol. 52, no. 4, pp. 475–503, 2014.

[2] M. Doumiati *et al.*, "Integrated vehicle dynamics control via coordination of active front steering and rear braking," *Eur. J. Control*, vol. 19, no. 2, pp. 121–143, 2013.

[3] T. Sardarmehni, H. Rahmani, and M. B. Menhaj, "Robust control of wheel slip in anti-lock brake system of automobiles," *Nonlinear Dyn.*, vol. 76, no. 1, pp. 125–138, 2013.

[4] H. Jing, Z. Liu, and H. Chen, "A switched control strategy for antilock braking system with on/off valves," *IEEE Trans. Veh. Technol.*, vol. 60, no. 4, pp. 1470–1484, May 2001.

[5] R. D. Castro, R. E. Araújo, and D. Freitas, "Wheel slip control of EVs based on sliding mode technique with conditional integrators," *IEEE Trans. Ind. Electron.*, vol. 60, no. 8, pp. 3256–3271, Aug. 2013.

[6] W. Pasillas-Lépine, A. Loría, and M. Gerard, "Design and experimental validation of a nonlinear wheel slip control algorithm," *Automatica*, vol. 48, no. 8, pp. 1852–1859, 2012.

[7] A. Okyay, E. Cigeroglu, and S. Ç. Başlamışlı, "A new sliding-mode controller design methodology with derivative switching function for anti-lock brake system," *Proc. Inst. Mech. Eng. C, J. Mech. Eng. Sci.*, vol. 227, no. 11, pp. 2487–2503, 2013.

[8] Y. Li, J. Zhang, and C. Lv, "Robust control of anti-lock brake system for an electric vehicle equipped with an axle motor," SAE Tech. Paper 2014-01-0140, 2014.

[9] V. Ćirović and D. Aleksendrić, "Adaptive neuro-fuzzy wheel slip control," *Expert Syst. Appl.*, vol. 40, no. 13, pp. 5197–5209, 2013.

[10] Y. G. Tang, Y. Wang, and M. Y. Han, "Adaptive fuzzy fractional-order sliding mode controller design for antilock braking systems," *J. Dyn. Syst., Meas., Control*, vol. 138, no. 4, pp. 041008-1–041008-8. Apr. 2016.

[11] X. Liu, M. Li, and M. Xu, "Model-predictive-control-based novel anti-skid method for electric vehicles using the wheel acceleration and the motor torque," *Proc. Inst. Mech. Eng. D, J. Automobile Eng.*, vol. 230, no. 13, pp. 1780–1790, 2016.

[12] T. A. Johansen, I. Petersen, J. Kalkkuhl, and J. Ludemann, "Gain-scheduled wheel slip control in automotive brake systems," *IEEE Trans. Control Syst. Technol.*, vol. 11, no. 6, pp. 799–811, Nov. 2003.

[13] C. Lv, J. Zhang, Y. Li, D. Sun, and Y. Yuan, "Hardware-in-the-loop simulation of pressure-difference-limiting modulation of the hydraulic brake for regenerative braking control of electric vehicles," *Proc. Inst. Mech. Eng. D, J. Automobile Eng.*, vol. 228, no. 6, pp. 649–662, 2014.

[14] J. W. Ko, S. Y. Ko, I. S. Kim, D. Y. Hyun, and H. S. Kim, "Co-operative control for regenerative braking and friction braking to increase energy recovery without wheel lock," *Int. J. Automotive Technol.*, vol. 15, no. 2, pp. 253–262, 2014.

[15] C. Jo, J. Ko, H. Yeo, T. Yeo, S. Hwang, and H. Kim, "Cooperative regenerative braking control algorithm for an automatic-transmission-based hybrid electric vehicle during a downshift," *Proc. Inst. Mech. Eng. D, J. Automobile Eng.*, vol. 226, no. 4, pp. 457–467, 2011.

[16] C. Lv, J. Zhang, and Y. Li, "Extended-Kalman-filter-based regenerative and friction blended braking control for electric vehicle equipped with axle motor considering damping and elastic properties of electric powertrain," *Vehicle Syst. Dyn.*, vol. 52, no. 11, pp. 1372–1388, 2014.

[17] X. Huang and J. Wang, "Model predictive regenerative braking control for lightweight electric vehicles with in-wheel motors," *Proc. Inst. Mech. Eng. D, J. Automobile Eng.*, vol. 226, no. 9, pp. 1220–1232, 2012.

[18] B. Wang, X. Huang, J. Wang, X. Guo, and X. Zhu, "A robust wheel slip ratio control design combining hydraulic and regenerative braking systems for in-wheel-motors-driven electric vehicles," *J. Franklin Inst.*, vol. 352, no. 2, pp. 577–602, Feb. 2015.
[19] R. de Castro, R. E. Araújo, M. Tanelli, S. Savaresi, and D. Freitas, "Torque blending and wheel slip control in EVs with in-wheel motors," *Vehicle Syst. Dyn.*, vol. 50, no. 1, pp. 71–94, Jul. 2012.
[20] W. Xiang, P. C. Richardson, C. Zhao, and S. Mohammad, "Automobile brake-by-wire control system design and analysis," *IEEE Trans. Veh. Technol.*, vol. 57, no. 1, pp. 138–145, Jan. 2008.
[21] F. Zhang, J. Xi, and R. Langari, "Real-time energy management strategy based on velocity forecasts using V2V and V2I communications," *IEEE Trans. Intell. Transp. Syst.*, vol. 18, no. 2, pp. 416–430, Feb. 2017.
[22] D. Jia and D. Ngoduy, "Enhanced cooperative car-following traffic model with the combination of V2V and V2I communication," *Transp. Res. B, Methodol.*, vol. 90, pp. 172–191, Aug. 2016.
[23] X. Zhu, H. Zhang, and Z. Fang, "Speed synchronization control for integrated automotive motor–transmission powertrain system with random delays," *Mech. Syst. Signal Process.*, vols. 64–65, pp. 46–57, Dec. 2015.
[24] X. Zhu, H. Zhang, J. Wang, and Z. Fang, "Robust lateral motion control of electric ground vehicles with random network-induced delays," *IEEE Trans. Veh. Technol.*, vol. 64, no. 11, pp. 4985–4995, Nov. 2015.
[25] U. Kiencke and L. Nielsen, *Automotive Control Systems: For Engine, Driveline, and Vehicle*. Berlin, Germany: Springer, 2005.
[26] R. De Castro, R. Araújo, and D. Freitas, "Optimal linear parameterization for on-line estimation of tire-road friction," *IFAC Proc. Vols.*, vol. 44, no. 1, pp. 8409–8414, 2011.

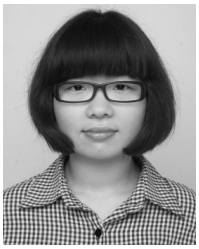

WEI LI received the B.E. and Ph.D. degrees from the Department of Aircraft Design Engineering, Northwestern Polytechnical University, Xi'an, China, in 2009 and 2015, respectively. From 2012 to 2014, she was a Visiting Scholar with the Department of Mechanical Engineering, Northwestern University, Evanston, IL, USA. She is currently with the School of Logistical Engineering, Shanghai Maritime University, China. Her current research interests include robust design, reliability engineering, and system safety.

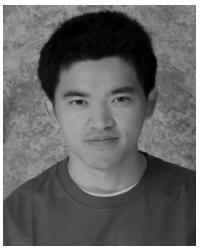

XIAOYUAN ZHU received the B.E. and Ph.D. degrees in mechanical engineering from Northwestern Polytechnical University, Xi'an, China, in 2009 and 2015, respectively. From 2012 to 2014, he was a Visiting Scholar with the Department of Mechanical and Aerospace Engineering, The Ohio State University, Columbus, OH, USA. He is currently with Merchant Marine College, Shanghai Maritime University, China. His current research interests include e-drive systems, powertrain systems, and wind and wave energy. He serves as a Guest Editor for *Advances in Mechanical Engineering*. He also serves as an Outstanding Reviewer for *Mechanical System and Signal Processing*, *ISA Transactions*, and *Neurocomputing*.

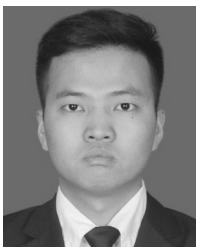

JI JU received the master's degree from the College of Information Engineering, Shanghai Maritime University, China. His research interests are vehicle dynamics and control.